THE JOURNAL OF BIOLOGICAL CHEMISTRY VOL. 285, NO. 38, pp. 29286–29294, September 17, 2010

A Minimal Cysteine Motif Required to Activate the SKOR K^+ Channel of *Arabidopsis* by the Reactive Oxygen Species H_2O_2*[S]

Received for publication, May 5, 2010, and in revised form, June 28, 2010 Published, JBC Papers in Press, July 6, 2010, DOI 10.1074/jbc.M110.141176

Carlos Garcia-Mata[‡1], Jianwen Wang[§], Pawel Gajdanowicz[¶], Wendy Gonzalez[‖], Adrian Hills[‡], Naomi Donald[‡], Janin Riedelsberger[¶], Anna Amtmann[‡], Ingo Dreyer[¶], and Michael R. Blatt[‡2]

From the [‡]Laboratory of Plant Physiology and Biophysics, Faculty of Biomedical and Life Sciences, Plant Sciences, University of Glasgow, Glasgow G12 8QQ, Scotland, United Kingdom, the [§]School of Pharmaceutical Sciences, Soochow University, Suzhou 215123, China, the [¶]Universität Potsdam, Institut für Biochemie und Biologie, Heisenberg-Group BPMPB, Karl-Liebknecht-Strasse 24/25, Haus 20, D-14476 Golm, Germany, and the [‖]Centro de Bioinformática y Simulación Molecular, Universidad de Talca, Casilla 721, Talca, Chile

Reactive oxygen species (ROS) are essential for development and stress signaling in plants. They contribute to plant defense against pathogens, regulate stomatal transpiration, and influence nutrient uptake and partitioning. Although both Ca^{2+} and K^+ channels of plants are known to be affected, virtually nothing is known of the targets for ROS at a molecular level. Here we report that a single cysteine (Cys) residue within the Kv-like SKOR K^+ channel of *Arabidopsis thaliana* is essential for channel sensitivity to the ROS H_2O_2. We show that H_2O_2 rapidly enhanced current amplitude and activation kinetics of heterologously expressed SKOR, and the effects were reversed by the reducing agent dithiothreitol (DTT). Both H_2O_2 and DTT were active at the outer face of the membrane and current enhancement was strongly dependent on membrane depolarization, consistent with a H_2O_2-sensitive site on the SKOR protein that is exposed to the outside when the channel is in the open conformation. Cys substitutions identified a single residue, Cys^{168} located within the S3 α-helix of the voltage sensor complex, to be essential for sensitivity to H_2O_2. The same Cys residue was a primary determinant for current block by covalent Cys *S*-methioylation with aqueous methanethiosulfonates. These, and additional data identify Cys^{168} as a critical target for H_2O_2, and implicate ROS-mediated control of the K^+ channel in regulating mineral nutrient partitioning within the plant.

Reactive oxygen species (ROS)[3] are major signals in virtually every aspect of eukaryotic cell biology (1, 2). In animals, they are important regulators of cell division and muscle contraction among others (3), and in plants they are essential for development (4) and stress signaling, including drought (5, 6) and defense against pathogens (7). Within proteins, ROS target a small subset of amino acids, notably cysteine (Cys) residues, chemically modifying these amino acids and thereby altering protein structure and function (8). Nonetheless, the targeted residues and associated motifs are often poorly defined, the effects wide ranging and protein-specific, thus confounding molecular analyses. Indeed, among the few well documented examples, ROS modifications in mammalian ryanodine-receptor and BK channels have different consequences depending on the positions of the residues targeted (3, 9).

For development and signaling in plants, the activities of membrane ion channels are essential, often including their regulation by ROS. For example, ROS affect non-selective cation channels during *Fucus* development (10); they regulate Ca^{2+} channels and Ca^{2+}-based signaling (5) as well as voltage-sensitive K^+ channels of guard cells (11) that are important for stomatal movement; they contribute in responses to drought and pathogen defense (12); and they have been implicated in targeting K^+ efflux during programmed cell death (13). However, until now virtually nothing has been known of the molecular targets for ROS in plants, nor has a site of action been identified with an ion channel protein.

SKOR is one of two K^+ channels found in *Arabidopsis thaliana* that rectify strongly outward, thereby mediating K^+ efflux from the cell. It is expressed within the xylem parenchyma of the root where it facilitates K^+ loading into the xylem (14), thereby contributing directly to K^+ homeostasis and indirectly, through charge balance, to the transport of other solutes throughout the plant (12, 15). Like other members of the Kv-like channel superfamily (16), the functional channel assembles from four monomers with each SKOR monomer incorporating six transmembrane α-helices. The first four α-helices form a positively charged voltage-sensor complex or "paddle" that moves within the membrane in response to voltage and couples this movement to the channel gate. The fifth and sixth α-helices line the aqueous pore through the membrane and assemble in a diaphragm or "gate" at the inner membrane surface, which opens/closes to regulate ion flux through the channel. Here we report that K^+ current through the heterologously expressed SKOR is modulated by H_2O_2, thereby identifying the K^+ channel as a potential target for ROS, and we show that a single Cys within the voltage sensor complex is essential for its ROS sen-

* This work was supported by National Science Foundation of China Grant 30772731 (to J. W.), a Heisenberg Fellowship (to I. D.), Deutsche Akademische Austausch Dienst/Consejo Nacional de Investigaciones Científicas y Técnicas Grant "NiaPoc" (to I. D. and W. G.), a Max Planck Research School "Primary Metabolism and Plant Growth" studentship (to J. R.), Biotechnology and Biological Sciences Research Council Grant BB/D001528/1, and a John Simon Guggenheim Memorial Fellowship (to M. R. B.).

[S] The on-line version of this article (available at http://www.jbc.org) contains supplemental Fig. S1.

[1] Present address: Institutos de Investigaciones Biologicas, Universidad Nacional de Mar del Plata, 7600 Mar del Plata, Buenos Aires, Argentina.

[2] To whom correspondence should be addressed. Tel.: 44-0-141-330-4771; Fax: 44-0-141-330-4447; E-mail: m.blatt@bio.gla.ac.uk.

[3] The abbreviations used are: ROS, reactive oxygen species; MTS, methanethiosulfonate; MMTS, methyl methanethiosulfonate; MTSES, sodium (2-sulfonatoethyl)-methanethiosulfonate; MTSEA, methanethiosulfonate ethylammonium chloride; DTNB, 5,5′-dithiobis(nitrobenzoic acid); TAPS, 3-{[2-hydroxy-1,1-bis(hydroxymethyl)ethyl]amino}-1-propanesulfonic acid.

sitivity. This Cys and adjacent sequences form a motif that shows extensive conservation among outward-rectifying Kv-like K^+ channels, but only from land plants, suggesting that the motif may represent an important regulatory target specialized for the habit of plants in dry environments.

MATERIALS AND METHODS

Molecular Biology—Site mutations were generated in wild-type SKOR and the C-terminal deletion mutant SKOR-ΔK746 as described previously (17, 18), and mutants and wild-type SKOR were subcloned into the bicistronic expression vector pCIG2, which contains an internal ribosome entry site and an enhanced green fluorescent protein cassette. All clones were verified by sequencing.

Mammalian Cell Culture and Electrophysiology—Human embryonic kidney (HEK293) cells were grown at 37 °C under 5% CO_2 in Dulbecco's modified Eagle's medium (Sigma) with 10% (v/v) fetal calf serum, 2 mM L-glutamine, 1:1000 penicillin and streptomycin. Cells were transfected using PolyFect Transfection Reagent (Qiagen), subcultured for 2 days, and 12 h prior to recording, dispersed using trypsin and plated on fibronectin-coated coverslips. For recording, the coverslips were mounted in perfusion chambers on an Axiovert200 fluorescence microscope (Zeiss, Germany). Cells expressing the channels were selected by visual inspection for co-expression of GFP fluorescence.

Patch pipettes were pulled from Kimax51 capillaries (Kimble Products) in two stages to give tips with resistances of 2–5 megaohms. Standard pipette solutions contained (in mM) 130 K-gluconate, 1 NaCl, 10 HEPES, 5 EGTA, 2.1 $MgCl_2$, 2.8 $CaCl_2$ (= 0.1 μM free $[Ca^{2+}]$ (19)), 10 TAPS, 5 phosphocreatine, 1 Mg-ATP, 0.02 deltamethrin, pH 8. The bath solutions contained (in mM) 5 mM KCl, 185 mM mannitol, 1.8 $CaCl_2$, 1 $MgCl_2$, 10 glucose, 5 HEPES/KOH, pH 7.4. DTT, glutathione, and H_2O_2 were added directly to bath or pipette solutions. Methanethiosulfonate (MTS) reagents (Toronto Research), H_2O_2, and ATP stock solutions were prepared fresh for dilution to a final concentration. Currents were recorded using an Geneclamp 500B amplifier (Axon Instruments, Sunnyvale, CA) and voltage clamp driven using Henry III software (Y-Science, Glasgow, UK). Currents were recorded after filtering at 1 kHz and analyzed as described previously (17, 20). *Xenopus* oocytes were prepared, injected with cRNA, and currents were recorded as described previously (17, 18). Data are reported as mean ± S.E. as appropriate with significance determined by Student's *t* test or analysis of variance.

Plant Growth and K^+ Content Assays—Seeds of Col-0 wild-type *Arabidopsis* and the *skor* and *rhd2* mutants were sterilized and stored in the dark at 4 °C to vernalize. The seed was germinated on 0.5× Murashige and Skoog basal salts medium (21) under continuous white light at 50 μmol/m^2/s at 22 °C. After 6 days, germinated seedlings were transferred to 0.7% agar plates containing 0.5× Murashige and Skoog medium alone and with 40 and 80 mM NaCl and 0.1 and 0.5 mM H_2O_2. Plants were harvested after 14 days growth. Root and shoot material was separated, analyzed for fresh weight, dried for 7 days at 70 °C, and analyzed for dry weight, and the dry material extracted in 2 N HCl (20:1 w/v) for 7 days before analysis for K^+ and Na^+ content by flame spectrophotometry. Cation contents were expressed in concentrations assuming a 1:1 relationship between fresh weight and cellular volume.

Molecular Dynamic Simulations—Molecular dynamic simulation was performed using the NAMD program (22). Open and closed SKOR models were embedded within a lipid bilayer in a periodic boundary condition box with water molecules, K^+ and Cl^- ions, and was first optimized using energy minimization followed by equilibration at 298 K for 3 ns with a harmonic restraint of 0.5 kcal/mol $Å^2$ applied to the backbone atoms (see supplemental Fig. S1) (18).

RESULTS

SKOR harbors 11 Cys residues, of which eight locate within the cytosolic C terminus of the protein and two, Cys^{228} and Cys^{234}, are situated in the S5 α-helix lining the channel pore (Fig. 1*A*). A single Cys, Cys^{168}, was found in the S3 α-helix of the voltage sensor complex and appears highly conserved among outward-rectifying K^+ channels of land plants (Fig. 1*A*). Deletion of the C-terminal 83 residues of SKOR (SKOR-ΔK746), including two Cys, has no measurable effect on SKOR current or gating when heterologously expressed (17, 23). Both in this background and in wild-type, substitutions of either Cys^{228} or Cys^{234} individually were not tolerated, nor did these mutations yield currents when combined with Cys^{168} substitutions, alone or together (not shown). However, currents were recovered in SKOR mutants with C168S (SKOR-C168S) or with paired C228S/C234S (SKOR-C228S/C234S) substitutions. Like wild-type SKOR, these mutants gave currents on positive voltage steps with pronounced sigmoidal activation kinetics and a sensitivity to extracellular $[K^+]$ when expressed in HEK293 cells (Fig. 1*B*) and *Xenopus* oocytes (not shown), albeit with somewhat faster activation kinetics.

SKOR Current Is Enhanced by ROS—Wild-type SKOR current generally showed a slow decay throughout the 10–20 min of most recordings once in the whole cell configuration. We found that adding 1 mM H_2O_2 to the bath reversed this decay and 10 and 30 mM H_2O_2 further enhanced the steady-state current amplitude by 2- to near 4-fold (Fig. 2*A*). Current enhancement was accompanied by a decrease in the half-times for activation (Fig. 2*A*), consistent with an action on gating, and complementary results were obtained in oocytes (not shown). In each of 23 independent experiments expressing SKOR in HEK293 cells (Fig. 2*B*), the current increased from near 0.5 nA to 1.5–2 nA at a clamp voltage of +80 mV following additions of 10 mM H_2O_2. However, no measurable effects were observed on treatment with the larger molecular weight, Cys-reactive reagent 5,5′-dithiobis-2-nitrobenzoic acid (DTNB, Fig. 2*C*); in 5 experiments DTNB gave currents similar to control treatments with buffer alone (not shown). Similarly, no effect was observed with the membrane-permeant reagent phenylarsine oxide (not shown), which cross-links vicinal cysteines (20).

Current enhancement by H_2O_2 was saturable with an apparent K_d for H_2O_2 of 3.8 ± 0.6 mM (Fig. 2*B*). No appreciable decay was observed after subsequent washing with buffer alone (Fig. 2*C*), at least within the time frame of recordings, indicating a persistence of ROS action. However, the H_2O_2 enhancement of SKOR current was fully reversible in the presence of the reduc-

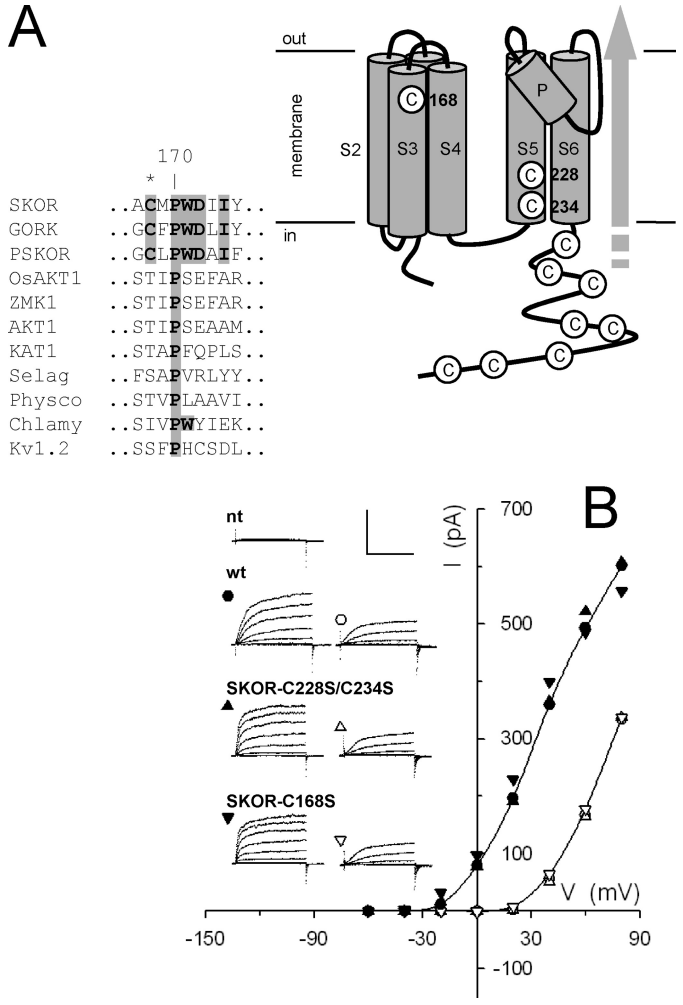

FIGURE 1. **The SKOR K^+ channel harbors 11 Cys residues, three of which are situated within the transmembrane domains of the protein.** *A*, schematic of the SKOR structure with positions of the Cys residues as indicated. Cys^{168}, located within the S3 α-helix of the S1–S4 voltage sensor complex, is highly conserved among outward-rectifying Kv-like channels of land plants. The *shaded arrow* indicates the position of the pore and K^+ flux within the tetrameric assembly of the functional channel. *Inset*: alignment of SKOR with representative outward-rectifying channels GORK (*Arabidopsis*), PSKOR (*Populus*), and inward-rectifying channels OsAKT1 (rice), ZMK1 (maize), AKT1 and KAT1 (*Arabidopsis*), and channels annotated for moss (*Physcomitrella patens*; Pp235474), liverwort (*Selaginella moellendorfii*; Sm406662), the alga *Chlamydomonas reinhardtii* (Cr144354), and with the mammalian Kv1.2 channel (for details, see Ref. 16, and NCBI and JDI/DOE databases). *Asterisk* indicates the conserved Cys and the adjacent motif shown in *bold with shading*. *B*, current-voltage characteristics of wild-type SKOR (●, ○) and mutants SKOR-C228S/C234S (▲, Δ) and SKOR-C168S (▼, ▽) expressed in HEK293 cells. Voltage clamp cycles from −80 mV to voltages between −60 and +80 mV. The current in each case was recorded from single cells bathed in 5 mM (*filled symbols*) and subsequently 100 mM K^+ (*open symbols*) and show the characteristic shift with external $[K^+]$ (16). *Insets,* representative current traces from a non-transfected HEK293 cell (*nt*), and from wild-type (*wt*), SKOR-C228S/C234S, and SKOR-C168S cross-referenced to the current-voltage plot by the symbols. *Scale*, horizontal, 2 s; vertical, 0.5 nA.

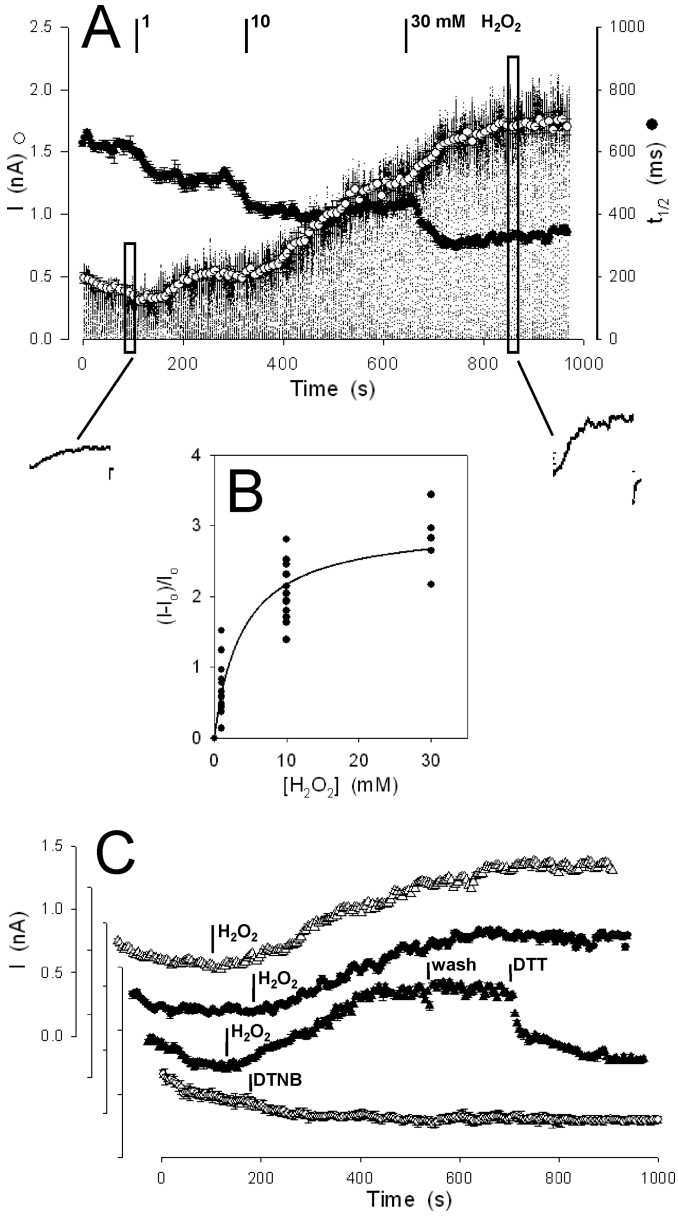

FIGURE 2. **SKOR current is reversibly enhanced by H_2O_2.** *A*, SKOR current recorded in one HEK293 cell during treatment with 1, 10, and 30 mM H_2O_2 and voltage clamped in repeated 5-s cycles of −50 mV holding (0.8 s), −80 mV conditioning (200 ms), +80 mV test (3 s), and −50 mV tailing (1 s) voltages. Mean ± S.E. are also shown for current amplitudes (○) calculated from the final 0.1 s of each test voltage step and for activation half-times ($t_{1/2}$, ●) determined after normalizing current relaxations. *Insets* (*below*), expanded current traces from individual clamp cycles taken just before addition of H_2O_2 and near the end of the experiment (indicated by the *boxed areas of the main trace*). *B*, mean increase in SKOR current amplitudes from all 23 experiments (cells) as a function of H_2O_2 concentration. Fitting to a simple hyperbolic function yielded an apparent K_d of 3.8 ± 0.6 and maximum 3.0 ± 0.2-fold enhancement. *C*, representative mean SKOR current enhancement in 10 mM H_2O_2 without (Δ) and with 10 mM glutathione in the patch pipette (●). Subsequent superfusion with buffer alone (wash) had no effect on the enhanced current, but the enhancement could be reversed by adding 10 mM DTT in the bath (▲). No SKOR current enhancement was seen after adding 10 mM DTNB (○) or buffer alone (not shown).

tant DTT when added subsequently to the bath (Fig. 2*C*). DTT had no effect when added inside by inclusion in the patch pipette, even when the DTT-containing pipette solutions were allowed to exchange with the cytosol for 5–6 min before adding H_2O_2 (not shown). Similarly, including reduced glutathione (GSH) at concentrations of 1, 5, and 10 mM in 6 experiments failed to suppress the effects of H_2O_2 on the SKOR current (Fig. 2*C*). These observations suggested that current enhancement depended on reversible oxidation of an isolated site (or sites) situated near the outer membrane surface and accessible to H_2O_2, but not to larger M_r redox reagents.

SKOR-C168S Is Insensitive to ROS—Because Cys^{168}, Cys^{228}, and Cys^{234} residues needed for functional expression of SKOR might be targets for H_2O_2, we examined ROS sensitivity of the

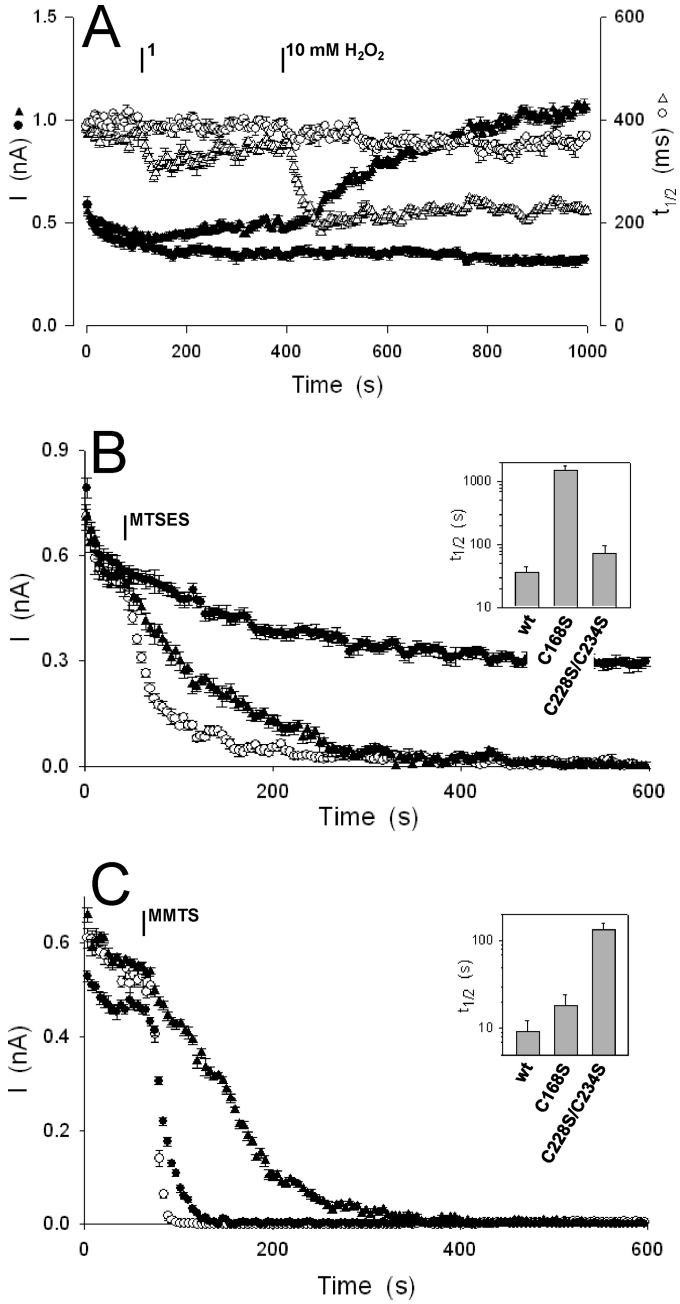

FIGURE 3. **The Cys^{168} residue is a principal target for H_2O_2 and *S*-methioylation by water-soluble MTS reagents.** *A*, current amplitudes (▲, ●) and activation half-times (Δ, ▲) of the SKOR-C228S/C234S (Δ, ▲) and SKOR-C168S (●, ○) during treatments with 1 and 10 mM H_2O_2. Voltage clamp cycles and analysis are as described in the legend Fig. 2. *B*, block of SKOR current by 400 μM MTSES. Current amplitudes of wild-type SKOR (○), SKOR-C228S/C234S (▲), and SKOR-C168S (●). *Inset*, mean half-times ($t_{1/2}$) for current block determined by non-linear least-squares fitting of current amplitudes after MTSES addition to a simple exponential decay function. Note the logarithmic scale. $t_{1/2}$ for buffer alone, 1280 ± 75 s ($n = 16$). *C*, block of SKOR current by 400 μM MMTS. Current amplitudes of wild-type SKOR (○), SKOR-C228S/C234S (▲), and SKOR-C168S (●). *Inset*, mean half-times ($t_{1/2}$) for current block determined by non-linear least-squares fitting of current amplitudes after MMTS addition to a simple exponential decay function. Note the logarithmic scale.

substitution mutants. In each of 12 experiments, SKOR-C228S/C234S showed essentially wild-type characteristics: current amplitude was enhanced in 1 and 10 mM H_2O_2 (Fig. 3*A*), and the response was reversed by adding DTT (not shown). Half-times for current activation of SKOR-C228S/C234S decreased on additions of H_2O_2 (Fig. 3*A*), and recovered with DTT treatments (not shown), much as was observed for wild-type SKOR. By contrast, in each of 11 experiments H_2O_2 failed to enhance the current carried by SKOR-C168S or to accelerate its activation, even with additions of 10 mM H_2O_2 (Fig. 3*A*). We cannot rule out more subtle effects of the ROS associated with other sites within the channel protein. Nonetheless, loss of sensitivity in SKOR-C168S led us to conclude that this residue is a major target for H_2O_2 action on the channel.

Substitution of Cys^{168} Confers Resistance to Current Block by S-Methioylation from Outside—We anticipated that the SKOR-C168S mutant might also be resistant to the effects of covalent Cys modification by MTS reagents. Methanethiosulfonates selectively attack cysteine thiols, rapidly *S*-methioylating the available Cys residues, and have been used to characterize the temporal and environmental accessibility of domains within many ion channels (*cf.* Refs. 16, 24, and 25). We made use of the lipid-soluble methyl methanethiosulfonate (MMTS) and the membrane impermeant (hydrophyllic) sodium (2-sulfonatoethyl)-methanethiosulfonate (MTSES) and methanethiosulfonate ethylammonium chloride (MTSEA), which carry negative and positive charges, respectively.

In each of 14 experiments, treatment of cells expressing wild-type SKOR with 400 μM MTSES (Fig. 3*B*) or MTSEA (not shown) blocked the current with kinetics well fitted to a simple exponential decay and half-times near 30 s (Fig. 3*B* and *inset*). These rates of block compare favorably with those for the voltage-dependent action of MTS reagents on the *Arabidopsis* KAT1 K^+ channel with Cys residues engineered in the S4 α-helix (25) and for block by *S*-methioylation of endogenous Cys in mammalian pacemaker channels (24). Similar results were obtained in recordings of SKOR-C228S/C234S, although the mutant showed a slower rate of current decay with MTS additions. Compared with the half-time for bath exchange (3 s), these rates of current block suggested that sites within the channel were accessible to the MTS reagents only some fraction of the time. However, SKOR-C168S currents were unaffected by additions of these MTS reagents (Fig. 3*B* and *inset*) and yielded a nominal mean half-time for current decay statistically equivalent to that of currents from SKOR-expressing cells treated with buffer alone (not shown). By contrast, treatments with MMTS led to a rapid loss of current with wild-type SKOR essentially within the time scale of the bath exchange. A marginally slower block was evident in the SKOR-C168S mutant, but a significant slowing of current block was seen only with SKOR-C228S/C234S (Fig. 3*C* and *inset*). These findings underscore differential sensitivities of the two SKOR mutants to Cys *S*-methioylation, a resistance of SKOR-C168S to water-soluble MTS reagents from the outside, and SKOR-C228S/C234S to the lipid-soluble reagent, consistent with the idea that Cys^{168} is exposed to the aqueous phase at the outer surface of the membrane.

ROS Sensitivity of SKOR Is Voltage-dependent—Opening of the pore in Kv-like channels depends on rotation of the pore-lining S5 and S6 α-helices coupled to movement of the voltage sensor complex of the S1–S4 α-helices (26). Charged residues within the S4 α-helix are thought to help drive movement of the voltage sensor as the membrane is biased toward an inside-

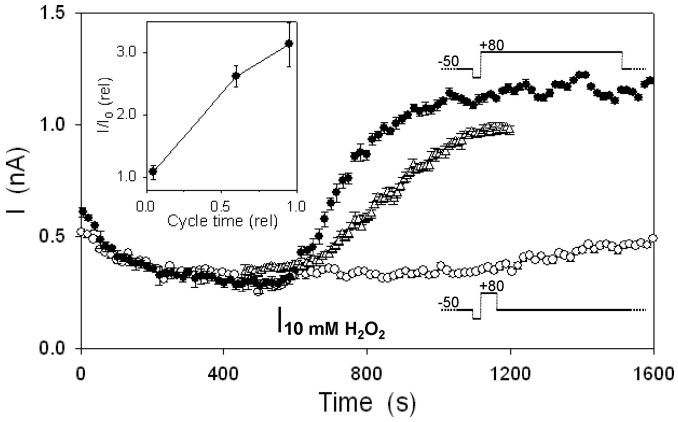

FIGURE 4. **SKOR current enhancement by H_2O_2 is voltage-dependent.** Time courses of current enhancement for SKOR expressed in HEK293 cells during treatments with 10 mM H_2O_2 and voltage clamped in trains of 20-s cycles with −50 mV holding (0.8 s), −80 mV conditioning (200 ms), +80 mV test, and −50 mV tailing voltages. Current amplitudes were determined as described in the legend to Fig. 2. Test and tailing voltage times were adjusted to give a normalized residence time at +80 mV of 0.05 (○) and 0.95 (●) as indicated (*schematic insets*, not to scale). Data using the clamp cycle train of Fig. 2 (Δ, normalized residence time at +80 mV, 0.6) were included for comparison. *Inset*, relative current enhancement as a function of relative cycle residence time at +80 mV.

positive electric field. Uncertainties about the extent of movement aside (27), this model fits remarkably well with the present understanding of plant K^+ channels (25, 28), and it raises a question whether access of H_2O_2 to Cys^{168}, and, hence, the sensitivity of SKOR to the ROS, might be voltage-dependent. Indeed, sequence alignments and homology mapping of SKOR to Kv1.2 (16, 18) place Cys^{168} close to the S3–S4 linker within the S3 α-helix of the voltage sensor, and thus near the outer surface of the membrane.

To test the voltage dependence of SKOR sensitivity to external H_2O_2, we used a simple extended protocol of 20 s, cycling repeatedly between −50 and +80 mV as before. In this case, the cycles were varied (Fig. 4, *schematic insets*) to give relative time distributions of 0.95:0.05 at voltages favoring either channel opening (+80 mV) or closing (−50 mV). In control experiments, both protocols yielded similar SKOR currents and activation kinetics (not shown). However, adding 10 mM H_2O_2 yielded very different results depending on time-averaged balance of clamp voltages (Fig. 4). With the balance of clamp voltages favoring the open channel at +80 mV, adding H_2O_2 gave a rapid enhancement of the SKOR current, analogous to the effects observed previously (Fig. 2). By contrast, with the time-averaged balance of clamp voltage favoring the closed channel at −50 mV, adding H_2O_2 showed only marginal enhancement of the current over the subsequent 10–15 min of recording. Similar results were obtained in each of 6 independent experiments and showed a near-proportional dependence of current enhancement in H_2O_2 as a function of the time fraction at voltages opening the channel (Fig. 4, *inset*), consistent with a voltage-dependent change in accessibility of the H_2O_2-sensitive site during SKOR gating.

ROS-dependent K^+ Partitioning Is Suppressed in the skor Mutant of Arabidopsis—SKOR plays an important role in K^+ loading of the xylem and its delivery to the shoot by the transpiration stream; the *skor* null mutation reduces K^+ content of the shoot and affects partitioning of other mineral nutrients within the plant (14) including Na^+, probably through its influence on charge balance across the plasma membrane of cells of the xylem parenchyma (15, 29). Reactive oxygen species and related signals also affect translocation of K^+ and other mineral nutrients to the shoot (30–32). We reasoned that if the ROS dependence of K^+ partitioning is mediated by SKOR, then deletion of the K^+ channel should suppress the associated changes in K^+ distribution to the shoot in the presence of Na^+ and exogenous H_2O_2.

To test this idea we grew wild-type *Arabidopsis* and mutants *skor* (14) and *rhd2* on 0.5× Murashige and Skoog basal salts medium (21) alone, with 40 and 80 mM NaCl and 0.1 and 0.5 mM H_2O_2. The *rhd2* mutant is impaired in NADPH oxidase activity and suppresses stress-induced ROS production and associated changes in nutrient transport, although wild-type characteristics are recovered with exogenous H_2O_2 (32). Thus, we anticipated the effects on K^+ partitioning to mirror that of the *skor* mutant. Fig. 5 summarizes data for tissue K^+ concentrations and K^+/Na^+ ratios in the wild-type, *skor*, and *rhd2* mutant *Arabidopsis* lines assayed 8 days after transfer to fresh medium alone and with the additions of NaCl and H_2O_2. We found that K^+ concentrations in shoot and root tissue of the wild-type plants increased with increasing NaCl in the medium although the K^+/Na^+ ratios decreased significantly, especially in the shoot, consistent with past observations (12, 33–35). Increasing H_2O_2 challenge had a similar, albeit much weaker effect. No significant differences were apparent in root K^+ concentrations or K^+/Na^+ ratios between wild-type and the mutant lines for any of the treatments. However, both mutants were severely impaired in K^+ partitioning to the shoot and in maintenance of K^+/Na^+ ratios. Consistent with previous studies (14), the *skor* mutant showed a 35% reduction in K^+ content when grown under standard conditions. More important, treatments with NaCl and H_2O_2 failed to promote the K^+ concentration in the shoot resulting in an attenuation in shoot K^+ content to ~50% of the wild-type in the presence of 80 mM NaCl and 0.5 mM H_2O_2. The *rhd2* mutant mirrored the *skor* phenotype under salt stress, displaying significantly lower shoot K^+ concentrations and K^+/Na^+ ratios than the wild-type plants. These results indicate (i) that SKOR and RHD2 affect partitioning of K^+ to the shoot, (ii) that both gene products are required for increasing shoot K^+ concentrations under salt stress, and (iii) that H_2O_2 mimics at least in part these effects on shoot K^+ concentration and K^+/Na^+ ratios with and without NaCl. We return to these points below.

DISCUSSION

Oxidation of Cys residues by H_2O_2 to form sulfenic acid effects post-translational modifications of proteins generally (1, 2), and has an important role in cellular signaling and control of membrane transport in plants (12). H_2O_2 and related ROS are important signals contributing to root development (4), homeostatic control of guard cell ion channels (5), and regulation of mineral and water flux during nutrient stress (15, 36). Nonetheless, identifying the molecular targets for ROS has proven difficult. Our studies now offer primary evidence that the SKOR K^+ channel of *Arabidopsis* is an important target for

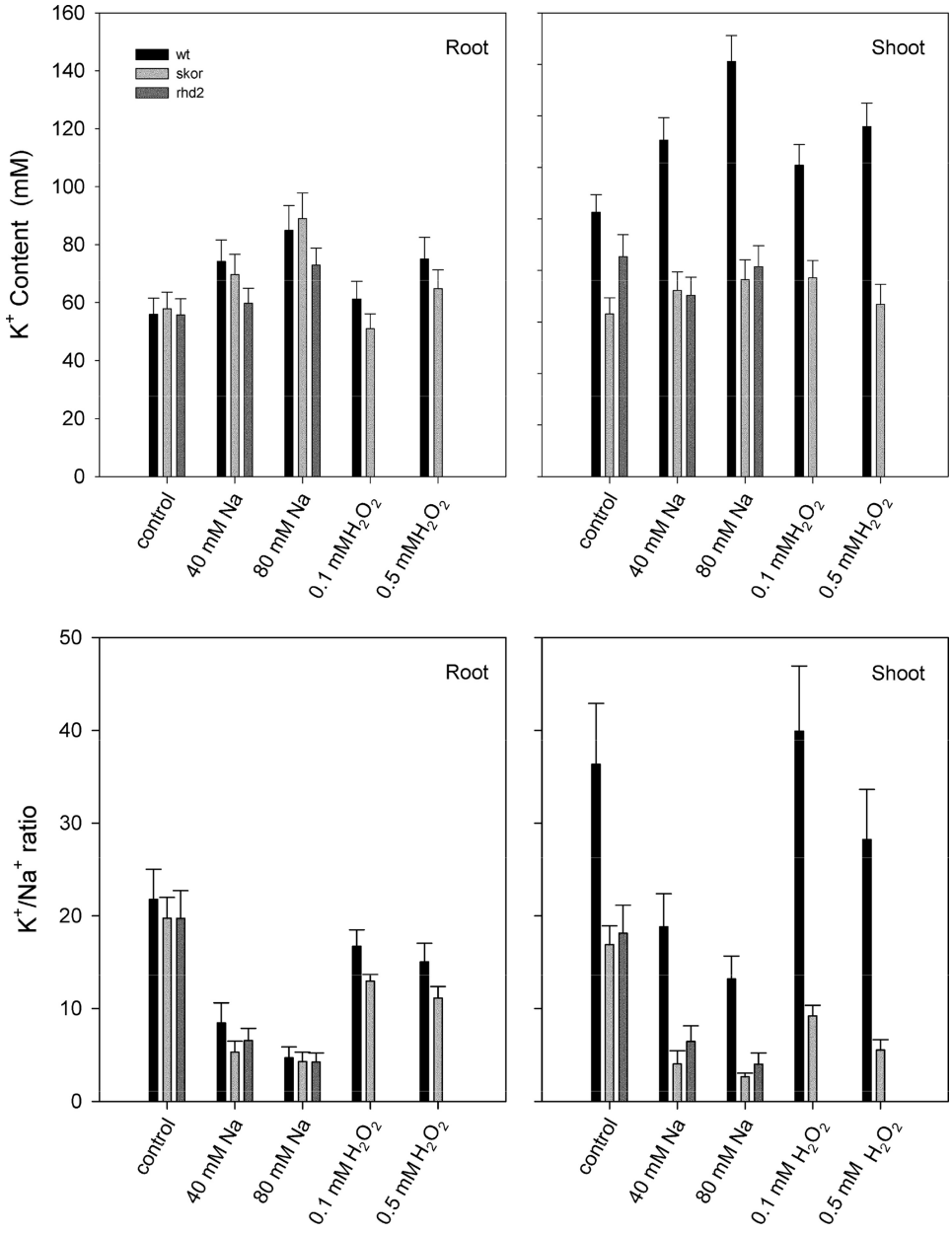

FIGURE 5. **The *skor* mutant of *Arabidopsis* suppresses ROS and salt stress-evoked changes in shoot K^+ content.** *Top*, total root and shoot K^+ content of *Arabidopsis* Col-O wild-type, *skor*, and *rhd2* mutant seeds grown for 14 days on 0.5× Murashige and Skoog alone and supplemented with 40 and 80 mM NaCl and 0.1 and 0.5 mM H_2O_2. Data are mean ±S.E. of three independent experiments (>10 plants each) and are expressed as concentrations based on measurements of fresh weight. *Bottom,* total root and shoot K^+/Na^+ ratios derived from the K^+ contents above and parallel measurements of Na^+ from the same tissue samples.

H_2O_2-mediated Cys modification, and they identify the Cys^{168} residue of the channel protein as the minimal requirement for channel regulation by the ROS. Because SKOR is a major pathway for K^+ transport into the xylem (14) and contributes to charge balance during the loading of other nutrients and metabolites, especially of anions such as NO_3^-, and their delivery via the transpiration stream, the findings also implicate a mechanistic link between stress-induced ROS production, nutrient partitioning, and long-distance signaling (12, 15, 31).

An Intrinsic Cys Defines the Voltage-dependent Sensitivity to External ROS—Central to identifying the SKOR Cys^{168} residue were discoveries that currents mediated by the wild-type K^+ channel expressed in HEK cells were reversibly enhanced by H_2O_2, showing a saturable dependence on its concentration, and that wild-type channel characteristics and sensitivity to H_2O_2 were retained in Cys-substitution mutants of SKOR except when the Cys^{168} site was replaced with serine (Figs. 2 and 3). This same Cys residue uniquely determined a predominant sensitivity of the K^+ channel to block by *S*-methioylation the water-soluble MTS reagents (Fig. 3). By contrast, SKOR-C228S/C234S showed a substantial rise in current amplitude in the presence of the ROS and, like the wild-type SKOR, was sensitive to MTSES and MTSEA. Because *S*-methioylation adds to the side chain bulk unlike H_2O_2-mediated oxidation, MTS modification was expected to introduce substantial steric constraints on protein conformation (16, 24, 25). This difference is the simplest explanation for the divergent effects of Cys modification. In either case, such specificity in Cys targeting by ROS is by no means unusual. For example, of the 100 Cys residues found in the ryanodine-receptor Ca^{2+} channel of muscle, only three are subject to modification from outside (3). Our observations do not rule out roles for one or more of the other 10 Cys residues of SKOR in control of the K^+ channel or its responses to other reactive species; however, they clearly identify Cys^{168} as a minimal and uniquely important residue needed for SKOR response to H_2O_2.

The significance of the Cys^{168} residue is underscored by the voltage dependence of SKOR enhancement by ROS. Homology mapping of SKOR to structures for the mammalian Kv1.2 K^+ channel (37) places Cys^{168} in SKOR close to the S3–S4 linker of the voltage sensor complex, and thus near the outer surface of the membrane. Positive voltage steps are thought to drive the voltage sensor outward during gating of SKOR, as in other plant Kv-like channels (16). So the parallel in voltage sensitivity of SKOR to H_2O_2 is entirely consistent with the idea that the exposure of Cys^{168} to ROS depends on displacement of the sensor in response to membrane voltage. It is of interest, too, that the SKOR current was responsive to DTT (M_r 154) from the outside, but not the inside of the membrane, and to water-soluble reagents MTSES (M_r 242) and MTSEA (M_r 192), but not to the

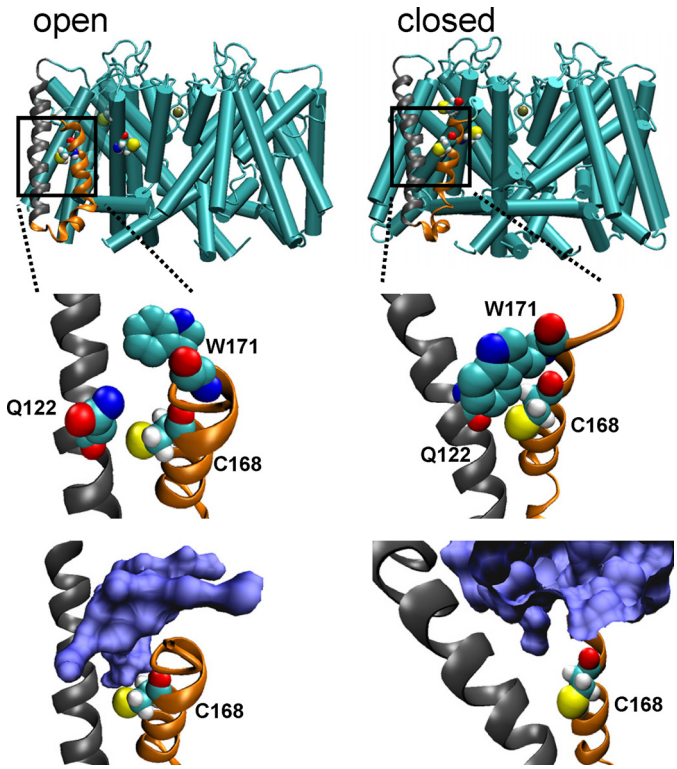

FIGURE 6. **Cys^{168} residue of SKOR is expected to reside in a water-filled pocket accessible from the outside in the open, but not in the closed conformation.** Results of molecular dynamic simulations are shown in a side-on view of the SKOR channel assembly (*top*) with S2 and S3 α-helices of one monomer in ribbon (*gray* and *orange*, respectively) and Cys^{168}, Cys^{228}, and Cys^{234} in van der Waals representations following equilibration (see supplemental Fig. S1). Expanded views of the S2 and S3 α-helices show amino acid residues (*center*) and the water-filled space in *blue* (*bottom*) adjacent to Cys^{168}. Protein structures were recorded every 10 ps and the root mean square deviation was calculated with the VMD trajectory tool (46) using α-C atoms to confirm equilibration. Root mean square deviation averages from 300 superimposed coordinates were determined at 10-ps intervals and gave a root mean square deviation of 0.863 ± 0.083 (±S.D.) in the open state and 0.457 ± 0.035 (±S.D.) in the closed state.

larger, aromatic compound DTNB (M_r 398). SKOR-C168S was also less effective in protecting against the lipid-soluble MMTS reagent by comparison with SKOR-C228S/C234S (Fig. 3). One simple explanation for this selectivity is that the sulfhydryl of Cys^{168} is situated within a water-filled pocket which, on depolarization, is exposed to the bulk solution outside through an aqueous gap small enough to exclude the larger water-soluble compound. Indeed molecular dynamic simulations, based on mapping to the Kv1.2 K^+ channel (18), are in agreement with this interpretation: they suggest that Cys^{168} is situated within a water pocket roughly 4.6 Å in diameter and 6.9 Å deep, large enough to accept H_2O_2, DTT, and MTS reagents, but too small to fit the aromatic DTNB, which connects to the outside with movement of the voltage sensor complex to the open state (Fig. 6 and supplemental Fig. S1). This interpretation agrees also with the lack of action of DTT or glutathione when introduced from the cytosolic face of the membrane.

It is of interest that the SKOR current was evident in Cys-substitution mutants retaining Cys^{168} or the Cys^{228}/Cys^{234} pair, but not in mutants incorporating single substitutions, either C228S or C234S, with or without the C168S mutation. The Cys^{228}/Cys^{234} pair are likely to be situated nearer the inner surface of the membrane, within the S5 α-helix and well removed from Cys^{168} (Fig. 5). Given the effect of the C228S/C234S substitutions in reducing current sensitivity to the lipid-soluble MMTS (Fig. 3*C*), these residues are probably buried within the membrane. It could be argued that covalent Cys^{228}–Cys^{234} linkage is important for protein structure, channel assembly, or coupling of the voltage gate. However, such an explanation falls foul of the observation that eliminating both Cys residues otherwise had little effect on the SKOR current. Nonetheless, the Cys^{228}/Cys^{234} pair are localized within a region of SKOR, which is recalcitrant to exchange with at least one other Kv-like channel from *Arabidopsis* (38) and may point to other functional requirements for these residues.

ROS Sensitivity and the Physiology of K^+ Partitioning—We note the extensive conservation of the Cys^{168} residue and adjacent sequence within S3 α-helices of other outward-rectifying Kv-like K^+ channels from angiosperms, but not in the Kv channels of algae or moss, nor of *Drosophila*, *Caenorhabditis elegans,* or mammals (Fig. 1*A*). The comparison raises the possibility that this motif reflects a set of unique adaptations of land plants to dry environments. Activation of SKOR by ROS does carry significant implications for the partitioning of K^+ and other charged species within the plant. For example, plant growth in nutrient-depleted soils requires efficient redistribution of assimilates within the plant (12), and shortages in K^+, NO_3^-, and PO_4^{2-} (15) as well as salt stress (39) all promote ROS production in plant roots. Furthermore, during water stress and in the presence of abscisic acid the delivery of K^+ and NO_3^- to the shoot occurs in association with substantial changes in xylem pH (31), root water permeability (40), increases in ROS (15), and over longer time periods, changes in the expression of SKOR and other ion channels (14, 41). How these processes are coordinated is still poorly understood, and their dissection remains a challenge.

Our findings support the proposed role for SKOR in charge balance and cation exchange (14, 15, 29) during solute transfer from root to shoot, and they point to a connection between this process and the consequences of ROS-mediated signals. We found that the *skor* mutant suppressed changes in K^+ content of the shoot, but not of the root under salt stress; furthermore, it showed a substantially reduced K^+/Na^+ ratio in the shoot even in the absence of elevated Na^+ outside, and this characteristic was evident also when the plants were exposed to exogenous H_2O_2 (Fig. 5). The reduced K^+/Na^+ ratio is particularly important, because it reflects the ability of the plant to balance the cation content. Previous reports have highlighted decreases in K^+ content following salt stress (*cf.* Refs. 33, 34 and 12 for review), but these studies have often drawn on short-term NaCl challenge and the effects of salt stress in reducing the K^+ content of the plant rather than the long-term effects on inorganic cation balance. Furthermore, the capacity to retain K^+ has been shown to be strongly dependent on the availability of K^+ as well as Ca^{2+} in *Arabidopsis* (33, 35) and many other species (for review see Ref. 12); we note that a numerical comparison of these data is more difficult simply because Ca^{2+} availability affects Na^+ uptake as well as the K^+/Na^+ ratio (33, 35), but the pattern of changes is consistent in each

case. Indeed, Shabala *et al.* (29) have reported that the K^+ content of barley xylem sap and shoots can increase in the presence of Na^+ although their results also show a substantial rise in Na^+ content so that the K^+/Na^+ ratio declined under these conditions. A previous study of *Arabidopsis* (33) has shown that the rate of Na^+ uptake by the roots is not affected in seedlings of the *skor* mutant, and at least one study of transporter gene expression has indicated a substantial (>1500%) rise in *SKOR* transcript abundance under salt stress (42). These findings are consistent with our observations of a longer term rise in shoot K^+ content, its loss in the *skor* mutant as well as a suppression of the shoot K^+/Na^+ ratio, and the corresponding insensitivity of root K^+ content and K^+/Na^+ ratios to the *skor* mutant (Fig. 5). Thus the findings highlight a role for the channel in cation exchange during solute transfer to the shoot, and they also serve to underscore the longer term adaptive capacity associated with the channel but most likely related to changes in its expression under stress.

That the *rhd2* mutant was similarly affected under salt stress, and that the *skor* mutant showed a greater sensitivity in the relative change in K^+/Na^+ ratio with H_2O_2 (Fig. 5), is also consistent with a role for ROS action on K^+/Na^+ exchange and K^+ partitioning to the shoot. Again, it is tempting to suggest a parallel between the effects of H_2O_2 on SKOR channel activity and of the *skor* and *rhd2* mutants on the K^+/Na^+ ratio and K^+ in the shoot and, again, the difficulty lies in temporal differences between the two sets of data: whereas the effects of ROS on the channel are mediated directly over a time scale of seconds to minutes, the cation contents of root and shoot reflect the cumulative effects of Na^+ stress and H_2O_2 over a period of days. Thus, we anticipate other mechanisms for ROS action on cation partitioning through changes in the expression of *SKOR* (42), HKT1, and other transporters that will come into play over longer time periods (32, 43–45). Our identification of a Cys residue critical for SKOR sensitivity to ROS now implicates a new dimension to this homeostatic network that may operate over time scales of seconds to minutes, and it offers a molecular "handle" with which to genetically manipulate and explore this dimension.

Acknowledgments—We thank Lorenzo Lamattina (Mar del Plata, Argentina) for support during preparation of this manuscript, John Christie and Pat Jones (Glasgow) for help with HEK293 cell cultures, Rafael Garcia-Mata (Chapel Hill) for the pCIG2 vector, and Gerhard Thiel (Darmstadt) for early guidance with HEK cell recordings. skor and rhd2 mutant seeds were generous gifts from Herve Sentenac (Montpellier) and Daniel Schachtman (St. Louis), respectively.

REFERENCES

1. Winterbourn, C. C., and Hampton, M. B. (2008) *Free Radic. Biol. Med.* **45,** 549–561
2. Salsbury, F. R., Jr., Knutson, S. T., Poole, L. B., and Fetrow, J. S. (2008) *Protein Sci.* **17,** 299–312
3. Aracena-Parks, P., Goonasekera, S. A., Gilman, C. P., Dirksen, R. T., Hidalgo, C., and Hamilton, S. L. (2006) *J. Biol. Chem.* **281,** 40354–40368
4. Foreman, J., Demidchik, V., Bothwell, J. H., Mylona, P., Miedema, H., Torres, M. A., Linstead, P., Costa, S., Brownlee, C., Jones, J. D., Davies, J. M., and Dolan, L. (2003) *Nature* **422,** 442–446
5. Kwak, J. M., Mori, I. C., Pei, Z. M., Leonhardt, N., Torres, M. A., Dangl, J. L., Bloom, R. E., Bodde, S., Jones, J. D., and Schroeder, J. I. (2003) *EMBO J.* **22,** 2623–2633
6. Wang, P., and Song, C. P. (2008) *New Phytol.* **178,** 703–718
7. Torres, M. A., Jones, J. D., and Dangl, J. L. (2006) *Plant Physiol.* **141,** 373–378
8. Stone, J. R., and Yang, S. P. (2006) *Antioxid. Redox Signal.* **8,** 243–270
9. Tang, X. D., Garcia, M. L., Heinemann, S. H., and Hoshi, T. (2004) *Nat. Struct. Mol. Biol.* **11,** 171–178
10. Coelho, S. M., Taylor, A. R., Ryan, K. P., Sousa-Pinto, I., Brown, M. T., and Brownlee, C. (2002) *Plant Cell* **14,** 2369–2381
11. Köhler, B., Hills, A., and Blatt, M. R. (2003) *Plant Physiol.* **131,** 385–388
12. Amtmann, A., and Blatt, M. R. (2007) in *Plant Solute Transport* (Yeo, A. R., and Flowers, T., eds) pp. 99–132, Blackwells, Oxford
13. Demidchik, V., Cuin, T. A., Svistunenko, D., Smith, S. J., Miller, A. J., Shabala, S., Sokolik, A., and Yurin, V. M. (2010) *J. Cell Sci.* **123,** 1468–1479
14. Gaymard, F., Pilot, G., Lacombe, B., Bouchez, D., Bruneau, D., Boucherez, J., Michaux-Ferrière, N., Thibaud, J. B., and Sentenac, H. (1998) *Cell* **94,** 647–655
15. Schachtman, D. P., and Shin, R. (2007) *Annu. Rev. Plant Biol.* **58,** 47–69
16. Dreyer, I., and Blatt, M. R. (2009) *Trends Plant Sci.* **14,** 383–390
17. Johansson, I., Wulfetange, K., Porée, F., Michard, E., Gajdanowicz, P., Lacombe, B., Sentenac, H., Thibaud, J. B., Mueller-Roeber, B., Blatt, M. R., and Dreyer, I. (2006) *Plant J.* **46,** 269–281
18. Gajdanowicz, P., Garcia-Mata, C., Gonzalez, W., Morales-Navarro, S. E., Sharma, T., González-Nilo, F. D., Gutowicz, J., Mueller-Roeber, B., Blatt, M. R., and Dreyer, I. (2009) *New Phytol.* **182,** 380–391
19. Föhr, K. J., Warchol, W., and Gratzl, M. (1993) *Methods Enzymol.* **221,** 149–157
20. Sokolovski, S., and Blatt, M. R. (2004) *Plant Physiol.* **136,** 4275–4284
21. Murashige, T., and Skoog, F. (1962) *Physiol. Plant.* **15,** 473–497
22. Phillips, J. C., Braun, R., Wang, W., Gumbart, J., Tajkhorshid, E., Villa, E., Chipot, C., Skeel, R. D., Kale, L., and Schulten, K. (2005) *J. Comp. Chem.* **26,** 1781–1802
23. Dreyer, I., Porée, F., Schneider, A., Mittelstädt, J., Bertl, A., Sentenac, H., Thibaud, J. B., and Mueller-Roeber, B. (2004) *Biophys. J.* **87,** 858–872
24. Xue, T., and Li, R. A. (2002) *J. Biol. Chem.* **277,** 46233–46242
25. Latorre, R., Olcese, R., Basso, C., Gonzalez, C., Munoz, F., Cosmelli, D., and Alvarez, O. (2003) *J. Gen. Physiol.* **122,** 459–469
26. Long, S. B., Campbell, E. B., and Mackinnon, R. (2005) *Science* **309,** 903–908
27. Tombola, F., Pathak, M. M., and Isacoff, E. Y. (2005) *Neuron* **48,** 719–725
28. Lai, H. C., Grabe, M., Jan, Y. N., and Jan, L. Y. (2005) *Neuron* **47,** 395–406
29. Shabala, S., Shabala, S., Cuin, T. A., Pang, J., Percey, W., Chen, Z., Conn, S., Eing, C., and Wegner, L. H. (2010) *Plant J.* **61,** 839–853
30. Armengaud, P., Breitling, R., and Amtmann, A. (2004) *Plant Physiol.* **136,** 2556–2576
31. Wilkinson, S., and Davies, W. J. (2002) *Plant Cell Environ.* **25,** 195–210
32. Shin, R., and Schachtman, D. P. (2004) *Proc. Natl. Acad. Sci. U.S.A.* **101,** 8827–8832
33. Essah, P. A., Davenport, R., and Tester, M. (2003) *Plant Physiol.* **133,** 307–318
34. Wang, B., Davenport, R. J., Volkov, V., and Amtmann, A. (2006) *J. Exp. Bot.* **57,** 1161–1170
35. Kaddour, R., Nasri, N., M'rah, S., Berthomieu, P., and Lachaâl, M. (2009) *Comptes. Rendus. Biologies* **332,** 784–794
36. Cuin, T. A., and Shabala, S. (2007) *Plant Cell Environ.* **30,** 875–885
37. Long, S. B., Campbell, E. B., and Mackinnon, R. (2005) *Science* **309,** 897–903
38. Riedelsberger, J., Sharma, T., Gonzalez, W., Gajdanowicz, P., Morales-Navarro, S. E., Garcia-Mata, C., Mueller-Roeber, B., González-Nilo, F. D., Blatt, M. R., and Dreyer, I. (2010) *Mol. Plant* **3,** 236–245
39. Xiong, L., Schumaker, K. S., and Zhu, J. K. (2002) *Plant Cell* **14,** S165–S183
40. Boursiac, Y., Boudet, J., Postaire, O., Luu, D. T., Tournaire-Roux, C., and Maurel, C. (2008) *Plant J.* **56,** 207–218
41. Pilot, G., Gaymard, F., Mouline, K., Chérel, I., and Sentenac, H. (2003) *Plant Mol. Biol.* **51,** 773–787

42. Maathuis, F. J. M. (2006) *J. Exp. Bot.* **57,** 1137–1147
43. Davenport, R. J., Muñoz-Mayor, A., Jha, D., Essah, P. A., Rus, A., and Tester, M. (2007) *Plant Cell Environ.* **30,** 497–507
44. Sunarpi, Horie, T., Motoda, J., Kubo, M., Yang, H., Yoda, K., Horie, R., Chan, W. Y., Leung, H. Y., Hattori, K., Konomi, M., Osumi, M., Yamagami, M., Schroeder, J. I., and Uozumi, N. (2005) *Plant J.* **44,** 928–938
45. Berthomieu, P., Conéjéro, G., Nublat, A., Brackenbury, W. J., Lambert, C., Savio, C., Uozumi, N., Oiki, S., Yamada, K., Cellier, F., Gosti, F., Simonneau, T., Essah, P. A., Tester, M., Véry, A. A., Sentenac, H., and Casse, F. (2003) *EMBO J.* **22,** 2004–2014
46. Humphrey, W., Dalke, A., and Schulten, K. (1996) *J. Mol. Graph.* **14,** 33–38